Underwater Localization and Mapping:

Observability Analysis and Experimental Results

Mohammadreza Bayat [1] and A. Pedro Aguiar [1,2] *

Abstract

Purpose - We investigate the observability properties of the process of simultaneous localization and mapping of an Autonomous Underwater Vehicle (AUV), a challenging and important problem in marine robotics, and illustrate the derived results through computer simulations and experimental results with a real AUV.

Design/methodology/approach - We address the single/multiple beacon observability analysis of the process of simultaneous localization and mapping of an Autonomous Underwater Vehicle (AUV) by deriving the nonlinear mathematical model that describes the process; then applying a suitable coordinate transformation, and subsequently a time-scaling transformation to obtain a Linear Time Varying (LTV) system. The AUV considered is equipped with a set of inertial sensors, a depth sensor, and an acoustic ranging device that provides relative range measurements to a set of stationary beacons. The location of the beacons do not need to be necessarily known and in that case, we are also interested to localize them. Numerical tests and experimental results illustrate the derived theoretical results.

Findings - We show that, if either the position of one of the beacons or the initial position of the AUV is known, then the system is at least locally weakly observable, in the sense that the set of indistinguishable states from a given initial configuration contains a finite set of isolated points. The simulations and experiments results illustrate the findings.

Originality/value - In the single and multiple beacon case and for manoeuvres with constant linear and angular velocities both expressed in the body-frame, known as trimming or steady-state trajectories, we derive conditions under which it is possible to infer the state of the resulting system (and in particular the position of the AUV). We also describe implementation of an advanced continuous time constrained minimum energy observer combined with multiple model techniques. Numerical tests and experimental results illustrate the derived theoretical results.

Keywords: Observability analysis, Minimum energy observers, Range measurements, Localization, Marine robotics.

*This work was supported in part by projects MORPH (EU FP7 under grant agreement No. 288704), CONAV/FCT-PT (PTDC/EEA-CRO/113820/2009), and the FCT [PEst-OE/EEI/LA0009/2011]. The first author benefited from a PhD scholarship of the Foundation for Science and Technology (FCT), Portugal. [1]Institute for Systems and Robotics (ISR), Instituto Superior Técnico (IST), Lisbon, Portugal. mbayat@isr.ist.utl.pt
[2]Faculty of Engineering, University of Porto (FEUP) , Porto, Portugal. pedro.aguiar@fe.up.pt

1 Introduction

The localization of an Autonomous Underwater Vehicle (AUV) is a challenging and important problem in marine robotics. Since electromagnetic signals do not propagate well below the sea surface, a variety of different approaches has been developed that make use of acoustic signals. Ultra Short BaseLine (USBL), Long BaseLine (LBL), and GPS Intelligent Buoy (GIB) are examples of underwater navigation and positioning systems where all use the concept of beacons, transponders, and range measurements taken from relative/absolute time of flight of acoustic signals (Kinsey et al. 2006).

Another promising and interesting approach is to use only one beacon for localization. One of the very first works on single beacon acoustic navigation can be traced back to (Scherbatyuk 1995), where a least-squares algorithm is proposed to find the unknown initial position and constant-velocity of an AUV moving in horizontal plane while affected by unknown constant current. In (Larsen 2000), the author describes a Synthetic Long Base-Line (SLBL) navigation algorithm, which makes use of a single LBL in combination with a high performance dead-reckoning navigation system. In (Casey & Hu 2007) the authors describe an Extended Kalman Filter (EKF) for localization of an AUV using a single beacon, and in (Saude & Aguiar 2009) combining the dead-reckoning information with multiple range measurements taken at different instants of time from the vehicle to a single beacon, a robust estimation algorithm was proposed for vehicle localization in the presence of unknown ocean currents. In (Olson et al. 2006), a range only beacon localization algorithm is presented, which assumes no prior knowledge of beacons' locations. A pure range only sub-sea Simultaneous Localization and Mapping (SLAM) has been designed in (Newman & Leonard 2003). Cooperative AUV navigation using a single manoeuvrings surface craft has been studied in (Fallon et al. 2009). Recently, the authors in (McPhail & Pebody 2009) describe a post-processing method for positioning a deep diving AUV using a set of acoustic ranges from a single beacon on a surface ship while the AUV executes a closed path under the ship. The approach was validated through experimental results. In (Webster et al. 2009), the authors present a formulation and evaluation of a centralized EKF navigation system for underwater vehicles, which employs Doppler sonar, depth sensors, synchronous clocks, and a single moving acoustic reference beacon. In (Webster et al. 2012), the readers can find a more extensive review of previous works in the area of single-beacon navigation.

Regarding the observability problem for single beacon AUV localization, one of the first works is reported in (Song 1999), where resorting to the Fisher information concept, a necessary and sufficient condition for local system observability is presented for two-dimensional manoeuvring target tracking with range-only measurements from a single observer. More extensively in (Gadre & Stilwell 2005, Gadre 2007), the authors have investigated the observability of the linearized single beacon navigation system. Another interesting study that reformulates the problem to a Linear Time Varying (LTV) system is reported in (Batista et al. 2010, 2011), where necessary and sufficient conditions on the observability are provided. In (Arrichiello et al. 2011), the authors investigated the nonlinear observability concepts of a nonlinear inter-vehicle ranging system using observability rank conditions. The results obtained are validated experimentally in an equivalent single beacon navigation scenario.

This work addresses the single/multiple beacon observability analysis of the process of simultaneous localization and beacon mapping for an AUV that uses range measurements to stationary beacons for navigation and with also the possibility of using depth measurements. To this effect, we first apply a coordinate transformation similar to the one presented in (Aguiar & Hespanha 2006) and then a time-scaling transformation to obtain a LTV system. Then, we investigate for the case that the motion of the AUV corresponds to constant linear and angular velocities expressed in the body-frame, (also known as trimming or steady-state trajectories), under which conditions it is possible to reconstruct the initial state of the resulting system (and in particular the position of the AUV). Comparing to the works mentioned above, there are two main differences in this paper: i) we focus on obtaining conditions expressed in the body frame of the AUV, which usually are more meaningful, and ii) we address the multiple beacon case. We show that if either the position of one of the beacons or the initial position of the AUV is known, then the system is at least locally weakly observable, in the sense that the set of indistinguishable states from a given initial configuration contains a finite set of isolated points. Numerical tests and experimental results illustrate the results derived. To this end, the implementation of an advanced continuous time constrained minimum energy observer combined with multiple model techniques is described.

The paper is organized as follows: Section 2 formulates the process model of single/multiple beacon system. The observability analysis of the proposed system is investigated in Section 3. In Section 4 we present the structure of the observer used to estimate the state of the system followed by simulations and experimental results conducted with the Medusa underwater vehicle. Concluding remarks are given in Section 5.

2 Process Model

In this section we investigate the observability conditions of the problem of computing in real time an estimate of the position of an AUV and simultaneously constructing a map of beacons in its surrounding. The map whose building process is based on ranging measurements obtained from stationary acoustic modems (beacons) contains an estimate of the location of the beacons. To formulate the process model we consider two coordinate frames: fixed earth or inertial coordinate frame $\{\mathcal{I}\}$, and body fixed coordinate frame $\{\mathcal{B}\}$ that is attached to the AUV, which moves with respect to the coordinate frame $\{\mathcal{I}\}$. Let $({}^{\mathcal{I}}\boldsymbol{p}_{\mathcal{B}}, {}^{\mathcal{I}}_{\mathcal{B}}\mathcal{R}) \in SE(3)$ be the configuration of the frame $\{\mathcal{B}\}$ with respect to $\{\mathcal{I}\}$, where ${}^{\mathcal{I}}\boldsymbol{p}_{\mathcal{B}}$ indicates the position of the AUV in frame $\{\mathcal{I}\}$, and ${}^{\mathcal{I}}_{\mathcal{B}}\mathcal{R}$ the rotation matrix from $\{\mathcal{B}\}$ to $\{\mathcal{I}\}$. The equations of motion can be written as

$$ {}^{\mathcal{I}}\dot{\boldsymbol{p}}_{\mathcal{B}} = {}^{\mathcal{I}}_{\mathcal{B}}\mathcal{R}\,\boldsymbol{\nu} \tag{1} $$

$$ {}^{\mathcal{I}}_{\mathcal{B}}\dot{\mathcal{R}} = {}^{\mathcal{I}}_{\mathcal{B}}\mathcal{R}\,S(\boldsymbol{\omega}) \tag{2} $$

where the linear and angular velocities $(\boldsymbol{\nu}, \boldsymbol{\omega} : [0, \infty) \to \mathbb{R}^3)$ are viewed as input signals to the system (1)-(2). In (2), $S(\cdot)$ is a function from $\mathbb{R}^3$ to the space of

skew-symmetric matrices $\mathbb{S} := \{M \in \mathbb{R}^{3\times 3} : M = -M'\}$ defined by

$$S(\boldsymbol{a}) := \begin{bmatrix} 0 & -a_3 & a_2 \\ a_3 & 0 & -a_1 \\ -a_2 & a_1 & 0 \end{bmatrix}$$

In what follows we will use the Euler angles $\boldsymbol{\eta} = [\phi, \theta, \psi]$ to parametrize the rotation matrix. Consider now n stationary beacons located at unknown positions ${}^{\mathcal{I}}\boldsymbol{q}_i$, $i \in \{1, 2, ..., n\}$, but assumed to be stationary, that is

$${}^{\mathcal{I}}\dot{\boldsymbol{q}}_i = 0 \tag{3}$$

For each $i \in \{1, 2, ..., n\}$ let $r_i(t)$ be an acoustic ranging measurement acquired at time t from the i^{th} beacon. In this case, the measurement or output model is given by

$$r_i = \left\| {}^{\mathcal{I}}\boldsymbol{q}_i - {}^{\mathcal{I}}\boldsymbol{p}_{\mathcal{B}} \right\| \tag{4}$$

$$z_i = [0, 0, 1]\,{}^{\mathcal{I}}\boldsymbol{q}_i \tag{5}$$

$$z_0 = [0, 0, 1]\,{}^{\mathcal{I}}\boldsymbol{p}_B \tag{6}$$

where z_0 is the depth of the AUV that is assumed to be available (we consider the practical situation that the AUV is equipped with a depth sensor). We also consider that the location of the beacons q_i are only unknown in the horizontal plane, that is, we assume that we know the depth z_i. This is a reasonable assumption if each beacon is attached to a buoy that is at the surface or the depth information is sent via the acoustic channel.

Equations (1)-(6) represent the process model of the problem of simultaneous localization and beacon mapping of the AUV. From the nonlinear system (1)-(6) we will now construct a new LTV system and derive under what conditions the new system is *equivalent* to (1)-(6). Note that once we have an LTV system we can apply the powerful tools of linear estimation theory for observability analysis. The strategy to obtain an LTV system does not follow the ones described in (Krener & Isidori 1983, Plestan & Glumineau 1997) but it is specific tailored for our application. The idea is to view the beacons q_i in body frame $\{\mathcal{B}\}$ and introduce a *virtual* beacon, $\boldsymbol{q}_0$, located at the origin of $\{\mathcal{I}\}$ (see Figure 1). Following this strategy and resorting to some of the ideas in (Aguiar & Hespanha 2006), we first express $\boldsymbol{q}_0$ in $\{\mathcal{B}\}$ as

$${}^{\mathcal{B}}\boldsymbol{q}_0 = {}^{\mathcal{I}}_{\mathcal{B}}\mathcal{R}'\,{}^{\mathcal{I}}\boldsymbol{q}_0 - {}^{\mathcal{I}}_{\mathcal{B}}\mathcal{R}'\,{}^{\mathcal{I}}\boldsymbol{p}_{\mathcal{B}}$$

and compute its dynamic equation given by

$$\begin{aligned} {}^{\mathcal{B}}\dot{\boldsymbol{q}}_0 &= {}^{\mathcal{I}}_{\mathcal{B}}\dot{\mathcal{R}}'\,({}^{\mathcal{I}}\boldsymbol{q}_0 - {}^{\mathcal{I}}\boldsymbol{p}_{\mathcal{B}}) + {}^{\mathcal{I}}_{\mathcal{B}}\mathcal{R}'\,{}^{\mathcal{I}}\dot{\boldsymbol{q}}_0 - {}^{\mathcal{I}}_{\mathcal{B}}\mathcal{R}'\,{}^{\mathcal{I}}\dot{\boldsymbol{p}}_{\mathcal{B}} \\ &= -S(\boldsymbol{\omega})\,{}^{\mathcal{B}}\boldsymbol{q}_0 - \boldsymbol{\nu} \end{aligned}$$

where we have used (3). To obtain the dynamics of the position of the other beacons $\boldsymbol{q}_i$ in body frame, we introduce the vector $\boldsymbol{p}_i$ that connects the virtual beacon $\boldsymbol{q}_0$ to $\boldsymbol{q}_i$. Note that ${}^{\mathcal{I}}\boldsymbol{p}_i$ is a stationary vector while ${}^{\mathcal{B}}\boldsymbol{p}_i$ is in general a time dependent vector (with the same magnitude of ${}^{\mathcal{I}}\boldsymbol{p}_i$ but rotated by ${}^{\mathcal{I}}_{\mathcal{B}}\mathcal{R}'$). Therefore,

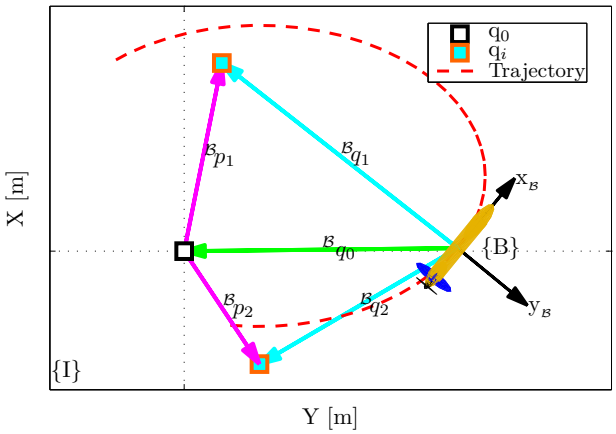

Figure 1: Illustration of representative state vectors in 2D space.

$$
\begin{aligned}
{}^{\mathcal{B}}\boldsymbol{p}_i &= {}^{\mathcal{B}}\boldsymbol{q}_i - {}^{\mathcal{B}}\boldsymbol{q}_0 \\
{}^{\mathcal{B}}\dot{\boldsymbol{p}}_i &= -S(\boldsymbol{\omega})\,{}^{\mathcal{B}}\boldsymbol{p}_i
\end{aligned}
\tag{7}
$$

From (4), (7), and using the fact that ${}^{\mathcal{I}}\boldsymbol{q}_i = {}^{\mathcal{I}}\boldsymbol{p}_{\mathcal{B}} + {}^{\mathcal{I}}_{\mathcal{B}}\mathcal{R}\,{}^{\mathcal{B}}\boldsymbol{q}_i$ the measurement model can be written as

$$
r_i = \left\|{}^{\mathcal{I}}\boldsymbol{q}_i - {}^{\mathcal{I}}\boldsymbol{p}_{\mathcal{B}}\right\| = \left\|{}^{\mathcal{I}}_{\mathcal{B}}\mathcal{R}\,{}^{\mathcal{B}}\boldsymbol{q}_i\right\| = \left\|{}^{\mathcal{B}}\boldsymbol{p}_i + {}^{\mathcal{B}}\boldsymbol{q}_0\right\|
$$

where we have used, in the last equality, the fact that $\mathcal{R}$ is a orthogonal matrix. Defining the scalar state variable $\chi_i = \left\|{}^{\mathcal{B}}\boldsymbol{p}_i + {}^{\mathcal{B}}\boldsymbol{q}_0\right\|$, $i \in \{1, 2, ..., n\}$, the output equation (4) becomes $r_i = \chi_i$ where χ_i satisfies

$$
\begin{aligned}
\dot{\chi}_i &= \frac{\left({}^{\mathcal{B}}\boldsymbol{p}_i + {}^{\mathcal{B}}\boldsymbol{q}_0\right)' S(\boldsymbol{\omega})\left({}^{\mathcal{B}}\boldsymbol{p}_i + {}^{\mathcal{B}}\boldsymbol{q}_0\right) - \boldsymbol{\nu}'\left({}^{\mathcal{B}}\boldsymbol{p}_i + {}^{\mathcal{B}}\boldsymbol{q}_0\right)}{\chi_i} \\
&= \frac{-\boldsymbol{\nu}'({}^{\mathcal{B}}\boldsymbol{p}_i + {}^{\mathcal{B}}\boldsymbol{q}_0)}{r_i}
\end{aligned}
$$

Using the equalities ${}^{\mathcal{I}}\boldsymbol{q}_i = {}^{\mathcal{I}}_{\mathcal{B}}\mathcal{R}\,{}^{\mathcal{B}}\boldsymbol{p}_i$ and ${}^{\mathcal{I}}\boldsymbol{p}_B = -{}^{\mathcal{I}}_{\mathcal{B}}\mathcal{R}\,{}^{\mathcal{B}}\boldsymbol{q}_0$ we can write the output equation (5) and (6) as

$$
\begin{aligned}
z_i &= [0, 0, 1]\,{}^{\mathcal{I}}_{\mathcal{B}}\mathcal{R}\,{}^{\mathcal{B}}\boldsymbol{p}_i \\
z_0 &= -[0, 0, 1]\,{}^{\mathcal{I}}_{\mathcal{B}}\mathcal{R}\,{}^{\mathcal{B}}\boldsymbol{q}_0
\end{aligned}
$$

In summary we obtain an LTV system described by

$$
\begin{cases}
\dot{\boldsymbol{x}}(t) = A_{\boldsymbol{u},\boldsymbol{y}}(t)\boldsymbol{x}(t) + \boldsymbol{b}_{\boldsymbol{u}}(t) \\
\boldsymbol{y}(t) = C_{\boldsymbol{u}}(t)\boldsymbol{x}(t)
\end{cases}
\tag{8}
$$

where

$$
\begin{aligned}
\boldsymbol{x} &:= \left[\begin{array}{cccccccc} {}^{\mathcal{B}}\boldsymbol{q}_0', & {}^{\mathcal{B}}\boldsymbol{p}_1' & \dots & {}^{\mathcal{B}}\boldsymbol{p}_n', & \chi_1 & \dots & \chi_n \end{array}\right]' \\
\boldsymbol{y} &:= \left[\begin{array}{cccccccc} r_1 & \dots & r_n, & z_0, & z_1 & \dots & z_n \end{array}\right]' \\
\boldsymbol{u} &:= \left[\begin{array}{ccc} \boldsymbol{\nu}' & \boldsymbol{\omega}' & \boldsymbol{\eta}' \end{array}\right]' \\
\boldsymbol{s} &:= \left[\begin{array}{cccc} \frac{1}{r_1} & \frac{1}{r_2} & \dots & \frac{1}{r_n} \end{array}\right]' \\
A_{\boldsymbol{u},\boldsymbol{y}} &:= -\left[\begin{array}{ccc} S(\boldsymbol{\omega}) & \mathbf{0} & \mathbf{0} \\ \mathbf{0} & I_n \otimes S(\boldsymbol{\omega}) & \mathbf{0} \\ \boldsymbol{s} \otimes \boldsymbol{\nu}' & diag(\boldsymbol{s}) \otimes \boldsymbol{\nu}' & \mathbf{0} \end{array}\right] \\
\boldsymbol{b}_{\boldsymbol{u}} &:= \left[\begin{array}{ccc} -\boldsymbol{\nu}' & \mathbf{0} & \mathbf{0} \end{array}\right]' \\
C_{\boldsymbol{u}} &:= \left[\begin{array}{ccc} \mathbf{0} & \mathbf{0} & I_n \\ -[0,0,1]\,{}^{\mathcal{I}}_{\mathcal{B}}\mathcal{R}(\boldsymbol{\eta}) & \mathbf{0} & \mathbf{0} \\ \mathbf{0} & I_n \otimes \left([0,0,1]\,{}^{\mathcal{I}}_{\mathcal{B}}\mathcal{R}(\boldsymbol{\eta})\right) & \mathbf{0} \end{array}\right]
\end{aligned}
$$

and it should satisfy the algebraic constraint:

$$
\chi_i^2 = \left\| {}^{\mathcal{B}}\boldsymbol{p}_i + {}^{\mathcal{B}}\boldsymbol{q}_0 \right\|^2 \tag{9}
$$

In the above model, given two matrices $M_i \in \mathbb{R}^{m_i \times n_i}$, $i \in \{1, 2\}$ and a vector $v \in \mathbb{R}^n$, we denote by $M_1 \otimes M_2 \in \mathbb{R}^{m_1 n_1 \times m_2 n_2}$ the Kronecker product of M_1 by M_2 , and by $diag(v)$ the diagonal $n \times n$ matrix with the elements of v on the main diagonal. Moreover, $\mathbf{0}$ and I_n denote appropriate dimension matrix with all elements zero and $n \times n$ identity matrix respectively.

We remark that (8) is not defined when $r_i = 0$, which corresponds to the particular case that the position of the AUV coincides with the location of the i^{th} beacon. Notice also that we have introduced the equality constraint (9) on the states of the derived LTV system, and this fact has to be considered in the subsequent observability analysis.

3 Observability Analysis

SLAM is a technique to build an estimate of the environment map (within a complete unknown environment or with some a priori knowledge of the environment), while simultaneously compute an estimate of the position of the vehicle. Unless there is an *anchor* that relates the relative localization with the global (inertial) position, the process in (8), where ${}^{\mathcal{B}}\boldsymbol{q}_0$ can be viewed as the position of the AUV and the rest of the states correspond to beacons positions, is not observable. In fact the idea is to use a priori knowledge of one of the states and estimate the other unknown ones. For example, one assumption is to consider that the initial condition of the location of the AUV is known (which can be done in practice if the AUV starts at the surface and there is GPS).

Using the above argument and considering *at this stage* only one beacon, $n = 1$, from (8) we obtain the single beacon system with squared range state χ_1^2 and output r_1^2 plus depth measurements, as follows

$$
\left\{\begin{array}{l} \dot{\boldsymbol{x}}(t) = \nu(t)\left(A_{\boldsymbol{u}}(t)\boldsymbol{x}(t) + \boldsymbol{b}\right) \\ \boldsymbol{y}(t) = C_{\boldsymbol{u}}(t)\boldsymbol{x}(t) \end{array}\right. \tag{10}
$$

where

$$\boldsymbol{x} := \left[\begin{array}{ccc} {}^{\mathcal{B}}\boldsymbol{q}_0' & {}^{\mathcal{B}}\boldsymbol{p}_1' & \chi_1^2 \end{array}\right]'$$

$$\boldsymbol{y} := \left[\begin{array}{ccc} r_1^2 & z_0 & z_1 \end{array}\right]'$$

$$\boldsymbol{u} := \left[\begin{array}{ccc} \boldsymbol{\nu}' & \boldsymbol{\omega}' & \boldsymbol{\eta}' \end{array}\right]'$$

$$A_{\boldsymbol{u}} := -\left[\begin{array}{ccc} S(\boldsymbol{\omega})/\nu & \mathbf{0} & \mathbf{0} \\ \mathbf{0} & S(\boldsymbol{\omega})/\nu & \mathbf{0} \\ [2,0,0] & [2,0,0] & 0 \end{array}\right]$$

$$\boldsymbol{b} := -\left[\begin{array}{cc} 1 & \mathbf{0} \end{array}\right]'$$

$$C_{\boldsymbol{u}} := \left[\begin{array}{ccccccc} 0 & 0 & 0 & 0 & 0 & 0 & 1 \\ \sin\theta & -\sin\phi\cos\theta & -\cos\phi\cos\theta & 0 & 0 & 0 & 0 \\ 0 & 0 & 0 & -\sin\theta & \sin\phi\cos\theta & \cos\phi\cos\theta & 0 \end{array}\right]$$

with $\boldsymbol{\omega} = [\omega_1, \omega_2, \omega_3]'$, $\boldsymbol{\nu} = [\nu, 0, 0]'$, and ${}^{\mathcal{B}}\boldsymbol{q}_0 = [{}^{\mathcal{B}}q_{0,x}, {}^{\mathcal{B}}q_{0,y}, {}^{\mathcal{B}}q_{0,z}]'$.

At this point we introduce the following definitions adopted from (Hermann & Krener 1977, Nijmeijer & van der Schaft 1990).

Definition 1. *Given system* (10)*, we say that two initial conditions* $\boldsymbol{z}, \boldsymbol{z}'$ *are* indistinguishable *if the output-time histories* $\boldsymbol{y}$*, for a given admissible input* $\boldsymbol{u}$ *time series and satisfying the initial conditions* $\boldsymbol{x}(0) = \boldsymbol{z}$ *and* $\boldsymbol{x}(0) = \boldsymbol{z}'$ *are identical. For every* $\boldsymbol{z}$*, let* $\mathcal{I}\{\boldsymbol{z}\}$ *denote the set of all initial conditions that are indistinguishable from* $\boldsymbol{z}$*. The system* (10) *is* observable at z *if* $\mathcal{I}(z) = \{z\}$*, and is* observable *if* $\mathcal{I}(z) = \{z\}$ *for every possible* z *in the state space. The system* (10) *is* locally weakly observable at z *if* z *is an isolated point of* $\mathcal{I}(z)$ *and is* locally weakly observable *if it is locally weakly observable for every possible* z *in the state space.*

Remark 1. *In* (10) *we have considered squared ranging measurement to simplify the observability analysis. This does not change the observability results. In fact if we conclude that* (10) *is observable with a given input* $\boldsymbol{u}^*$ *in the sense that for every pair of distinct initial conditions* $(\boldsymbol{x}_0, \boldsymbol{z}_0)$ *there exists a time interval* $t \in [t^*, t_f]$*,* $t^* \geq 0$ *such that the corresponding squared range outputs are different*

$$y(t; \boldsymbol{u}^*, \boldsymbol{x}_0) := r_1^2(t; \boldsymbol{u}^*, \boldsymbol{x}_0) \neq y(t; \boldsymbol{u}^*, \boldsymbol{z}_0) := r_1^2(t; \boldsymbol{u}^*, \boldsymbol{z}_0)$$

Then it also follows that $r_1(t; \boldsymbol{u}^*, \boldsymbol{x}_0) \neq r_1(t; \boldsymbol{u}^*, \boldsymbol{z}_0)$*, which implies that the initial conditions* $(\boldsymbol{x}_0, \boldsymbol{z}_0)$ *for the original system (using ranges) will produce different outputs. The same can be concluded for local weak observability.* □

Remark 2. *For observability analysis we can consider without loss of generality that the linear velocity* $\boldsymbol{\nu}$ *does not include any non null term in* y *and* z *components. If this is not the case (e.g., there is side-slip in steady state), then instead of using the body fixed frame* $\{\mathcal{B}\}$ *to obtain the process model* (10) *we use the* flow frame $\{\mathcal{F}\}$*, which its origin coincides with* $\{\mathcal{B}\}$ *but the orientation is such that the linear velocity expressed in* $\{\mathcal{F}\}$ *is* $\boldsymbol{\nu}(t) = [\nu(t), 0, 0]'$*. Note that in this case the orientation* $\boldsymbol{\eta}$ *is with respect to* $\{\mathcal{F}\}$*.* □

Returning to the single beacon system, we start to re-write (10) in a standard LTV system by applying a time scale transformation with $\dot{\tau} = \nu(t)$, assuming

$\nu(t) \neq 0$. In this case, we obtain

$$\begin{aligned} \frac{d\boldsymbol{x}(\tau)}{d\tau} &= A_{\boldsymbol{u}}(\tau)\boldsymbol{x}(\tau) + b_{\boldsymbol{u}}(\tau) \\ \boldsymbol{y}(\tau) &= C_{\boldsymbol{u}}(\tau)\boldsymbol{x}(\tau) \end{aligned} \tag{11}$$

where $\tau = \int_{t_0}^{t} \nu(s)ds$. Since (11) is a time scaled version of (10), then both systems are equivalent in the observability sense. Furthermore, without loss of generality we can set $\nu(t) = 1$ (only for observability analysis purposes) and work again with (10).

We are now ready to study the observability of the single beacon case. We will consider the case that the vehicle is in steady state motion, that is, the linear and angular velocities are constant. Moreover, we consider the case that the initial condition of the beacon ${}^{\mathcal{B}}\boldsymbol{p}_1(0)$ is known. Later we will investigate the dual case where the initial location of the AUV ${}^{\mathcal{B}}\boldsymbol{q}_0(0)$ is known but the position of the beacons are unknown.

Theorem 1. *Consider system* (10) *but with* $C = [\mathbf{0}, 1]$*, which means that there are no depth measurements available, and suppose that*

$$\|\boldsymbol{\omega}\| > |\omega_1| > 0 \tag{12}$$

Then, the system is observable. Moreover, if instead

$$\|\boldsymbol{\omega}\| > |\omega_1| = 0 \tag{13}$$

holds, then system (10) *together with the algebraic constraint* (9) *is locally weakly observable with set of indistinguishable initial conditions consisting of only two isolated points:*

$$\mathcal{I}_r(\boldsymbol{x}_0) = \left\{ \boldsymbol{x}_0, \boldsymbol{x}_0 - \begin{bmatrix} \frac{2\boldsymbol{\omega}\boldsymbol{\omega}'}{\boldsymbol{\omega}'\boldsymbol{\omega}}\left({}^{\mathcal{B}}\boldsymbol{q}_0(0) + {}^{\mathcal{B}}\boldsymbol{p}_1(0)\right) \\ \mathbf{0} \\ 0 \end{bmatrix} \right\} \tag{14}$$

Proof. Since we are assuming that the linear and angular velocities are constant, it turns out that system (10) without depth measurements is an LTI system. In this case, the first 4 rows of the associated observability matrix has the following form:

$$\mathcal{O}_r = \begin{bmatrix} 0 & 0 & 0 & 0 & 0 & 0 & \frac{1}{2} \\ -1 & 0 & 0 & -1 & 0 & 0 & 0 \\ 0 & -\omega_3 & \omega_2 & 0 & -\omega_3 & \omega_2 & 0 \\ \omega_2^2 + 2\omega_3^2 & -\omega_1\omega_2 & -\omega_1\omega_3 & \omega_2^2 + \omega_3^2 & -\omega_1\omega_2 & -\omega_1\omega_3 & 0 \end{bmatrix} \tag{15}$$

Note that the other rows are combinations of the first 4, and therefore it follows that (15) has rank 4 if (12) holds. Notice also that the first three columns are a combination of the second three columns, meaning that an initial anchor is required for observability of the system. Since we know the initial condition of the beacon, the set of indistinguishable initial conditions for ${}^{\mathcal{B}}\boldsymbol{q}_0$ shrinks to only ${}^{\mathcal{B}}\boldsymbol{q}_0(0)$ and thus the system is observable.

Now, if additionally $\omega_1 = 0$, meaning that condition (13) holds, the null space associated to the observability matrix is given by $Null(\mathcal{O}_r) = \mathcal{N}\boldsymbol{\alpha}$, where

$$\mathcal{N} = \begin{bmatrix} -1 & 0 & 0 & 0 \\ 0 & -1 & 0 & 0 \\ 0 & 0 & -1 & 0 \\ 1 & 0 & 0 & 0 \\ 0 & 1 & 0 & \omega_2 \\ 0 & 0 & 1 & \omega_3 \\ 0 & 0 & 0 & 0 \end{bmatrix} \tag{16}$$

and $\boldsymbol{\alpha} = [\alpha_1, \ldots, \alpha_4]' \in \mathbb{R}^4$. Thus, for a given input $\boldsymbol{u}$ time series and an initial condition $\boldsymbol{x}_0 \in \mathbb{R}^7$, all the points $\breve{\boldsymbol{x}}_0 = \boldsymbol{x}_0 + \mathcal{N}\boldsymbol{\alpha} \in \mathbb{R}^7$ are indistinguishable from $\boldsymbol{x}_0$. Since the initial condition of the beacon is known ${}^{\mathcal{B}}\breve{\boldsymbol{p}}_1(0) = {}^{\mathcal{B}}\boldsymbol{p}_1(0)$, it implies that $\alpha_1 = \alpha_2 = \alpha_3 = 0$. Moreover, notice that $\breve{\boldsymbol{x}}_0$ should satisfy the constraint (9), resulting that

$$\alpha_4 \in \left\{ 0, -\frac{2\boldsymbol{\omega}'\left({}^{\mathcal{B}}\boldsymbol{q}_0(0) + {}^{\mathcal{B}}\boldsymbol{p}_1(0)\right)}{\boldsymbol{\omega}'\boldsymbol{\omega}} \right\}$$

and therefore it can be concluded that $\mathcal{I}_r(\boldsymbol{x}_0)$ is the set defined in (14). Thus, system (10) combined with constraint (9) is locally weakly observable. □

We remark that the fact of introducing a new output to the system (in this case the depth measurement) will not change the observability results of Theorem 1 implying that if (12) holds then the system is observable with range and depth measurements. The following theorem shows that it is possible to shrink the set of indistinguishable points in (14) and achieve a less conservative result if we have also depth measurements.

Theorem 2. *Consider system* (10) *and suppose that*

$$\omega_3 \cos\phi_0 \neq -\omega_2 \sin\phi_0 \tag{17}$$

holds. Then the system is observable.

Proof. Using (2) we can confirm that $[0,0,1]\,{}^{\mathcal{I}}_{\mathcal{B}}\dot{\mathcal{R}}(\boldsymbol{\eta}_0) = [0,0,1]\,{}^{\mathcal{I}}_{\mathcal{B}}\mathcal{R}(\boldsymbol{\eta}_0)S(\boldsymbol{\omega})$, which implies that the Observability matrix in this case takes the form

$$\mathcal{O}_z = \begin{bmatrix} -\begin{bmatrix} 0 & 0 & 1 \end{bmatrix} {}^{\mathcal{I}}_{\mathcal{B}}\mathcal{R}(\boldsymbol{\eta}_0) & & \mathbf{0} & 0 \\ & \mathbf{0} & & \\ & & \begin{bmatrix} 0 & 0 & 1 \end{bmatrix} {}^{\mathcal{I}}_{\mathcal{B}}\mathcal{R}(\boldsymbol{\eta}_0) & 0 \end{bmatrix}$$

where all the other rows are zero. Since (17) implies that (12) or (13) holds and in Theorem 1 we have computed the observability matrix of system (10) with range only measurement, we can now intersect the null space (16) with the null space of $\mathcal{O}_z$. It can be seen that if the condition (17) holds, the intersection of the null spaces contains only the origin, implying that $\alpha_4 = 0$, $\mathcal{I}_{rz}(\boldsymbol{x}_0) = \{\boldsymbol{x}_0\}$, and consequently the system is observable. This completes the proof. □

In Theorem 1 we provided necessary conditions (12) for observability and local weak observability of range only system combined with constraint (9). By introducing depth measurements we have shown that we can achieve observability if condition (17) is satisfied. However if condition (17) does not hold,

the depth information does not add any information to drop the ambiguity of indistinguishable initial conditions. This leaves us to the following question: If condition (17) is not satisfied, what are the observability properties for system (10) with range (and depth) measurements? The next result discusses this case, which complements all the other cases that are not covered by the conditions introduced in Theorems 1-2.

Theorem 3. *Consider system* (10) *and suppose that*

$$\omega_3 \cos\phi = -\omega_2 \sin\phi \tag{18}$$

holds. Then, the system combined with constraint (9) *is locally weakly observable with*

$$\mathcal{I}_{rz}(\boldsymbol{x}_0) = \left\{ \boldsymbol{x}_0, \boldsymbol{x}_0 - \begin{bmatrix} 2 \begin{bmatrix} 0 & 0 & 0 \\ 0 & c^2\phi_0 & -\cos\phi_0 s\phi_0 \\ 0 & -\cos\phi_0 s\phi_0 & s^2\phi_0 \end{bmatrix} \left({}^{\mathcal{B}}\boldsymbol{q}_0(0) + {}^{\mathcal{B}}\boldsymbol{p}_1(0) \right) \\ \mathbf{0} \\ 0 \end{bmatrix} \right\} \tag{19}$$

describing the set of indistinguishable points.

Proof. Condition (18) is a particular case. In fact, in this case the Euler angles rates satisfy

$$\begin{bmatrix} \dot{\phi} & \dot{\theta} & \dot{\psi} \end{bmatrix} = \begin{bmatrix} \omega_1 & \frac{\omega_2}{\cos\phi} & 0 \end{bmatrix} \tag{20}$$

Notice also that from the assumption of $\boldsymbol{\omega}$ being constant, using (18) we can conclude that either $\|\boldsymbol{\omega}\| = |\omega_1|$ or ϕ is constant. The later implies that $\dot{\phi} = 0$ and consequently from (20) that $\omega_1 = 0$. In this case, the corresponding observability matrix is

$$\mathcal{O}_{rz} = \begin{bmatrix} 0 & 0 & 0 & 0 & 0 & 0 & \frac{1}{2} \\ -1 & 0 & 0 & -1 & 0 & 0 & 0 \\ 0 & -\omega_3 & \omega_2 & 0 & -\omega_3 & \omega_2 & 0 \\ \omega_2^2 + \omega_3^2 & 0 & 0 & \omega_2^2 + \omega_3^2 & 0 & 0 & 0 \\ -\sin\theta_0 & \sin\phi_0 \cos\theta_0 & \cos\phi_0 \cos\theta_0 & 0 & 0 & 0 & 0 \\ 0 & 0 & 0 & -\sin\theta_0 & \sin\phi_0 \cos\theta_0 & \cos\phi_0 \cos\theta_0 & 0 \end{bmatrix}$$

Since (18) holds, the 3^{rd} and 4^{th} rows are combination of the other rows. The associated null space is $Null(\mathcal{O}_{rz}) = \mathcal{N}\boldsymbol{\alpha}$ where

$$\mathcal{N} = \begin{bmatrix} 0 & -s\phi_0 & -\cos\phi_0 \\ -\cos\phi_0 & -s\phi_0 & -\cos\phi_0 \\ s\phi_0 & 0 & 0 \\ 0 & s\phi_0 & \cos\phi_0 \\ 0 & s\phi_0 & 0 \\ 0 & 0 & s\phi_0 \\ 0 & 0 & 0 \end{bmatrix}$$

which does not depend on ω_1 and $\boldsymbol{\alpha} = [\alpha_1, \ldots, \alpha_3]' \in \mathbb{R}^3$. Imposing the constraint of knowing the initial condition of the beacon leads to $\alpha_2 = \alpha_3 = 0$.

Now, we have a first order linear subspace $\breve{\boldsymbol{x}} = \boldsymbol{x}_0 + \alpha_1[0, -\cos\phi_0, s\phi_0, 0, 0, 0]'$ and the algebraic state constraint described in (9). Solving the corresponding algebraic equation we find that

$$\alpha_1 \in \left\{0, 2[0, \cos\phi_0, -s\phi_0]\left({}^{\mathcal{B}}\boldsymbol{q}_0(0) + {}^{\mathcal{B}}\boldsymbol{p}_1(0)\right)\right\}$$

This implies that the set of indistinguishable points is restricted to only two isolated points defined in (19), thus the system is locally weakly observable. □

Until this point we have investigated the case where it is assumed that the initial location of the beacon, ${}^{\mathcal{B}}\boldsymbol{p}_1(0)$, is known and the initial position of the AUV, ${}^{\mathcal{B}}\boldsymbol{q}_0(0)$, is unknown. We now consider the dual case, that is, ${}^{\mathcal{B}}\boldsymbol{q}_0(0)$ is known but not the initial position of the beacon. The following result holds.

Theorem 4. *The system* (10) *with the assumption that* ${}^{\mathcal{B}}\boldsymbol{q}_0(0)$ *is known, has the same observability properties as the case where* ${}^{\mathcal{B}}\boldsymbol{p}_1(0)$ *is known in Theorems 1-3 but with the following set of indistinguishable points:*

Case of range only measurements:

$$\mathcal{I}_r(\boldsymbol{x}_0) = \left\{\boldsymbol{x}_0, \boldsymbol{x}_0 - \begin{bmatrix} \mathbf{0} \\ \frac{2\boldsymbol{\omega}\boldsymbol{\omega}'}{\boldsymbol{\omega}'\boldsymbol{\omega}}\left({}^{\mathcal{B}}\boldsymbol{q}_0(0) + {}^{\mathcal{B}}\boldsymbol{p}_1(0)\right) \\ 0 \end{bmatrix}\right\} \tag{21}$$

Case of range and depth measurements:

$$\mathcal{I}_{rz}(\boldsymbol{x}_0) = \left\{\boldsymbol{x}_0, \boldsymbol{x}_0 - \begin{bmatrix} \mathbf{0} \\ 2\begin{bmatrix} 0 & 0 & 0 \\ 0 & c^2\phi_0 & -\cos\phi_0 s\phi_0 \\ 0 & -\cos\phi_0 s\phi_0 & s^2\phi_0 \end{bmatrix}\left({}^{\mathcal{B}}\boldsymbol{q}_0(0) + {}^{\mathcal{B}}\boldsymbol{p}_1(0)\right) \\ 0 \end{bmatrix}\right\} \tag{22}$$

Proof. The proof for the case of range only measurements follows the same guidelines of Theorem 1 with the difference that we use the assumption ${}^{\mathcal{B}}\breve{\boldsymbol{q}}_0(0) = {}^{\mathcal{B}}\boldsymbol{q}_0(0)$. This concludes to $\mathcal{I}_r(\boldsymbol{x}_0)$ as presented in (21), which is a set of isolated points and thus the same results of Theorem 1 holds with the set defined in (21). Now by adding the depth measurement and taking into account condition (17), it follows that the intersection of (21) with the null space of $\mathcal{O}_z$ contains only $\boldsymbol{x}_0$ meaning that the system is observable and the results of Theorem 2 holds. Moreover, with the same reasoning as in Theorem 3, but with the assumption ${}^{\mathcal{B}}\breve{\boldsymbol{q}}_0(0) = {}^{\mathcal{B}}\boldsymbol{q}_0(0)$, we can conclude that the set of indistinguishable points consists of isolated points defined in (22). Thus, the system is locally weakly observable in this case. This completes the proof. □

We are now ready to state the observability result for system (8) which extends to the case with more than one beacon.

Theorem 5. *Consider system* (8) *with constant linear velocity* $\boldsymbol{\nu} \neq 0$ *and angular velocity* $\boldsymbol{\omega}$*. Suppose that there is an anchor, that is, the initial condition* ${}^{\mathcal{B}}\boldsymbol{q}_0(0)$ *or the position of one of the beacons* ${}^{\mathcal{B}}\boldsymbol{p}_i(0)$ *is known. Then the initial condition of other states can be reconstructed from the observed input and output pair* $\{\boldsymbol{u}(t), \boldsymbol{y}(t)\}$*,* $t \in [0, t_f)$*, provided that* (12) *holds when range measurements are available or* (17) *holds while range and depth measurements are available. Otherwise, the initial condition of each unknown vector in* $\left\{{}^{\mathcal{B}}\boldsymbol{q}_0, {}^{\mathcal{B}}\boldsymbol{p}_i; i \in \{1, 2, ..., n\}\right\}$ *has two possible solutions.*

Proof. For only one beacon the result follows from Theorems 1-4. Consider now more than one beacon. In this case it can be concluded from (8) that the dynamic equations of each pair $\{{}^{\mathcal{B}}\boldsymbol{p}_i, \chi_i\}$ does not depend on the other pairs. This means that the observability of the multiple beacon system can be investigated by analysing the observability of each single beacon system and therefore the result follows from Theorems 1-4. □

4 Simulation and Experimental Results

This section illustrates the observability results derived in the previous section. To this end, we present a high-performance observer of multiple model adaptive type and compare its behaviour both in simulation and by carrying out experimental tests with a real marine robotic vehicle.

4.1 Multiple Model Constrained Minimum Energy Observer

The observer used to test the observability results was introduced in (Bayat & Aguiar 2013) and the design methodology is inspired by (Aguiar & Hespanha 2003, 2006). Basically, the goal is to obtain an estimate of the state vector which minimizes the energy of the estimated noise and disturbance, while satisfying the equality algebraic constraint (9). More precisely, consider a continuous time system corrupted with additive deterministic but unknown bounded state disturbance $\boldsymbol{d}(t)$ and measurement noise $\boldsymbol{n}(t)$, where only discrete samples of observations are available:

$$\begin{cases} \dot{\boldsymbol{x}}(t) = A_{\boldsymbol{u},\boldsymbol{y}}(t)\boldsymbol{x}(t) + \boldsymbol{b}_{\boldsymbol{u}}(t) + G_{\boldsymbol{u}}(t)\boldsymbol{d}(t) \\ \boldsymbol{y}(t_k) = C_{\boldsymbol{u}}(t)\boldsymbol{x}(t_k) + \boldsymbol{n}(t_k) \end{cases} \tag{23}$$

The implemented multiple model Constrained Minimum Energy Estimator (CME) is composed by the following blocks:

Minimum Energy Estimator (ME)

The block depicted in Figure 2, solves the estimation problem for system (23) using the minimum energy estimation approach (Aguiar & Hespanha 2006, 2003), which is given by the following equations:

• For $t_{k-1} \leq t < t_k$, $k = 1, ..., k^*$, the ME continuous block computes predicted $\dot{\bar{\boldsymbol{x}}}(t)$, $\dot{Q}(t)$

$$\dot{Q}(t) = -A'_{\boldsymbol{u},\boldsymbol{y}}Q(t) - Q(t)A_{\boldsymbol{u},\boldsymbol{y}} - Q(t)G_{\boldsymbol{u}}R_{\boldsymbol{d}}G'_{\boldsymbol{u}}Q(t) \tag{24}$$

$$\dot{\bar{\boldsymbol{x}}}(t) = A_{\boldsymbol{u},\boldsymbol{y}}\bar{\boldsymbol{x}}(t) + \boldsymbol{b}_{\boldsymbol{u}} \tag{25}$$

• At $t = t_k$, $k = 1, ..., k^*$, the ME discrete block resets the integrators with

$$\begin{aligned} Q(t_k) &= Q(t_k^-) + C'_{\boldsymbol{u}}R_{\boldsymbol{n}}^{-1}C_{\boldsymbol{u}} \\ \bar{\boldsymbol{x}}(t_k) &= \bar{\boldsymbol{x}}(t_k^-) - Q(t_k)^{-1}C'_{\boldsymbol{u}}R_{\boldsymbol{n}}^{-1}\left(C_{\boldsymbol{u}}\bar{\boldsymbol{x}}(t_k^-) - y(t_k)\right) \end{aligned}$$

where $R_{\boldsymbol{d}} > 0$ and $R_{\boldsymbol{n}} > 0$ are weighting parameters on disturbance and measurement noises and the ME satisfies the initial conditions $Q(0) = Q_0 > 0$, $\bar{\boldsymbol{x}}(0) = \bar{\boldsymbol{x}}_0$, with $\bar{\boldsymbol{x}}_0$ denoting an initial estimate.

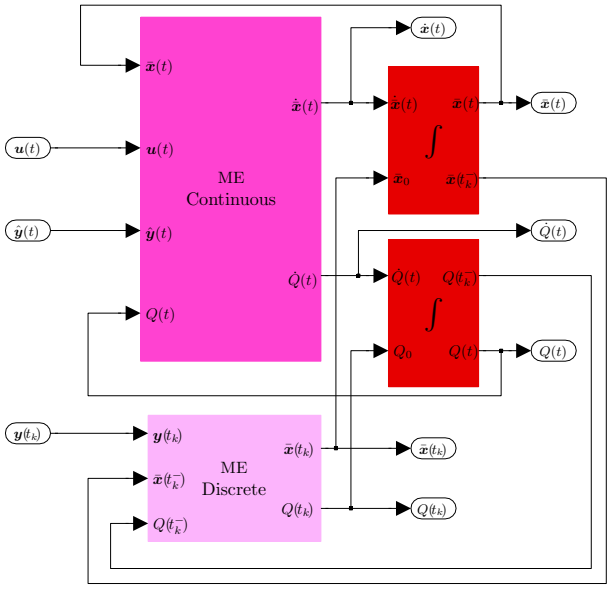

Figure 2: Block diagram of the ME used in the design of the CME observer.

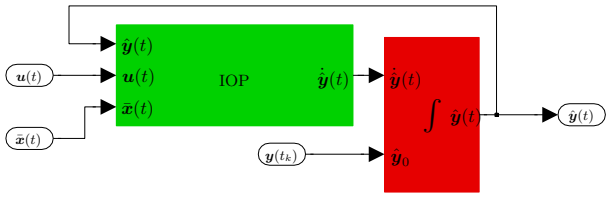

Figure 3: Block diagram of the IOP used in the design of the CME observer.

Inter-sample Output Predictor (IOP)

Notice that the observation $\boldsymbol{y}(t)$ used in (24)-(25) requires the assumption that the output of the system is a piecewise continuous signal in time, while in practice $\boldsymbol{y}$ is a discrete signal, which is available at times t_k, $k = 1, ..., k^*$. Thus, we use the concept of IOP, depicted in Figure 3, to reduce the model mismatch by predicting $\boldsymbol{y}(t)$ for $t_{k-1} \leq t < t_k$. For a general nonlinear system

$$\dot{\boldsymbol{x}} = f(\boldsymbol{x}, \boldsymbol{u}), \quad \boldsymbol{y} = h(\boldsymbol{x}, \boldsymbol{u})$$

the idea consists of using the predicted output computed by integrating

$$\dot{\hat{\boldsymbol{y}}}(t) = \frac{\partial \boldsymbol{h}(\hat{\boldsymbol{x}}, \boldsymbol{u})}{\partial \hat{\boldsymbol{x}}} \boldsymbol{f}(\hat{\boldsymbol{x}}, \boldsymbol{u}) \quad \forall t \in [t_{k-1}, t_k)$$

and reset at time t_k.

$$\hat{\boldsymbol{y}}(t_k) = \boldsymbol{y}(t_k)$$

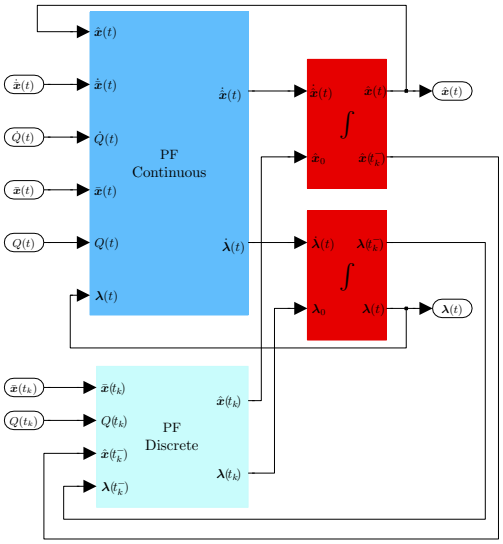

Figure 4: Block diagram of the PF used in the design of the CME observer.

Projection Filter (PF)

Since the solution obtained from the unconstrained state estimation problem, $\bar{\boldsymbol{x}}(t)$, does not necessarily satisfy the equality algebraic constraint (9), we use a PF, depicted in Figure 4, which acts as a weighted projection (with weighting matrix Q) from the state space of the system (8) ($\bar{\boldsymbol{x}}(t)$) to the space in which constraint (9) holds ($\hat{\boldsymbol{x}}(t)$). Notice that (9) can be written in a quadratic algebraic constraint form $\boldsymbol{z}'S_i\boldsymbol{z} = 0$. The PF is formulated as a constrained optimization problem with the Lagrangian function defined as

$$\mathcal{L}(\hat{\boldsymbol{x}}, \boldsymbol{\lambda}) = (\hat{\boldsymbol{x}} - \bar{\boldsymbol{x}})'Q(\hat{\boldsymbol{x}} - \bar{\boldsymbol{x}}) + \sum_{i=1}^{n} \lambda_i(\hat{\boldsymbol{x}}'S_i\hat{\boldsymbol{x}})$$

where $\boldsymbol{\lambda} \in \mathbb{R}^n$ is the Lagrange multiplier vector. Thus, the idea is to compute $\hat{\boldsymbol{x}}$ such that the sufficient KKT conditions for optimality of $\hat{\boldsymbol{x}}$ hold asymptotically in $[t_{k-1}, t_k)$ with

$$\begin{bmatrix} \dot{\hat{\boldsymbol{x}}} \\ \dot{\boldsymbol{\lambda}} \end{bmatrix} = \begin{bmatrix} \bar{Q} & \bar{S}(\hat{\boldsymbol{x}}) \\ \bar{S}(\hat{\boldsymbol{x}})' & 0 \end{bmatrix}^{-1} \left(\begin{bmatrix} -\dot{Q}\hat{\boldsymbol{x}} + Q\dot{\bar{\boldsymbol{x}}} + \dot{Q}\bar{\boldsymbol{x}} \\ 0 \end{bmatrix} - \mu \begin{bmatrix} Q(\hat{\boldsymbol{x}} - \bar{\boldsymbol{x}}) + \bar{S}(\hat{\boldsymbol{x}})\boldsymbol{\lambda} \\ \frac{1}{2}\bar{S}(\hat{\boldsymbol{x}})'\hat{\boldsymbol{x}} \end{bmatrix} \right)$$

computed by the PF continuous block. At t_k, the PF discrete block (see Figure 4) resets $\boldsymbol{\lambda}$ and $\hat{\boldsymbol{x}}$ with

$$\begin{bmatrix} \hat{\boldsymbol{x}}(t_k) \\ \boldsymbol{\lambda}(t_k) \end{bmatrix} = \begin{bmatrix} \bar{Q}^{-1}(t_k)Q(t_k)\bar{\boldsymbol{x}}(t_k) \\ \boldsymbol{\lambda}^*(t_k) \end{bmatrix}$$

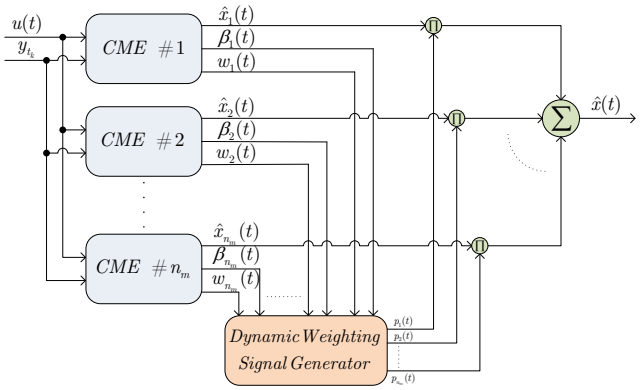

Figure 5: Block diagram of the designed MMAE.

Here $\boldsymbol{\lambda}^*(t_k)$ is given by solving $\boldsymbol{f}(\boldsymbol{\lambda}, t_k) = 0$ using the iterative generalized Newton's method, with

$$\begin{aligned} f_i(\boldsymbol{\lambda}, t_k) =& \bar{\boldsymbol{x}}' Q \bar{Q}^{-1} S_i \bar{Q}^{-1} Q \bar{\boldsymbol{x}}, \quad i \in \{1, 2, ..., n\} \\ \bar{Q} =& Q + \sum_{i=1}^{n} \lambda_i S_i \\ \bar{S}(\hat{\boldsymbol{x}}) =& [S_1 \hat{\boldsymbol{x}}, \ldots, S_n \hat{\boldsymbol{x}}] \end{aligned}$$

Multiple Model Adaptation

Notice that from the results in Section 3, we know that the process model (8) constrained by (9) is locally weakly observable in $[t_0, t_f]$ for some classes of inputs. In this case, the proposed CME initialized with $\bar{\boldsymbol{x}}(0)$ converges to the closest element of $\mathcal{I}(\boldsymbol{x}_0)$ in (14). However, as soon as the system becomes observable, the set of possible solutions consists of only one of them. This means that the observer initialized with any initial condition converges to a neighbourhood close the true initial condition, but notice that the time of convergence depends on how far is the initial estimate from the true initial condition ($\|\hat{\boldsymbol{x}}(0) - \boldsymbol{x}(0)\|$). In this case, to reduce the convergence time, a Multiple Model Adaptive Estimator (MMAE) scheme is proposed, see (Bayat & Aguiar 2013). To this effect, each CME is an observer initialized with a different initial condition and a weight signal $p_s(t)$, $s = 1, \ldots, n_m$, assigned to it. The weights are evaluated and updated at times t_k according to a weighting matrix $\mathcal{S}_s(t_k)$ and an error measuring function $w_s(t_k)$ that maps the observations of the system and the states of the each local observer to a non-negative real value (See Figure 5).

$$\hat{\boldsymbol{x}}(t) = \sum_{s=1}^{n_m} p_s(t_k)\hat{\boldsymbol{x}}_s(t), \quad \forall t \in [t_k, t_{k+1})$$

$$p_s(t_k) = \frac{p_s(t_{k-1})e^{-w_s(t_k)}}{\sum_{l=1}^{n_m} p_l(t_{k-1})e^{-w_l(t_k)}}, s \in \{1, 2, ..., n_m\}$$

$$w_s(t_k) = \frac{1}{2}\left\|\hat{\boldsymbol{y}}_s(t_k^-) - \boldsymbol{y}(t_k)\right\|^2_{\mathcal{S}_s(t_k)^{-1}}$$

$$\mathcal{S}_s(t_k) = C_{\boldsymbol{u}}(t_k)Q^{-1}(t_k)C'_{\boldsymbol{u}}(t_k) + R_{\boldsymbol{n}}$$

4.2 Simulation Results

To illustrate the derived observability results, we have simulated two scenarios:

- A 2D square type trajectory where the condition (18) holds except when the AUV is turning;
- A 3D helix type trajectory given by a constant pitch $\theta = (\frac{-\pi}{10})$ and turning rate $\boldsymbol{\omega} = [\tan(\frac{-\pi}{10})\frac{\pi}{50}, 0, \frac{\pi}{50}]'$, which means that conditions (12) and (17) hold.

In both scenarios, we consider three stationary beacons located at $[10, 10, 1]'$, $[-10, 10, 1]'$, $[3 - 10, 1]'$ as shown in Figures 6 and 7 with the symbol (◯). The AUV is moving with a constant forward speed of $0.5[m/s]$ starting from initial condition (□). To estimate the states of the undisturbed model introduced in (8) we use the proposed hybrid CME combined with MMAE approach. The models in the estimator are initialized with the same initial condition but different up to a sign in initial condition ${}^{\mathcal{B}}q_{i,y}(t_0), i \in \{1, 2, 3\}$.

As expected for the helix type trajectory the system is observable and therefore the estimate converges to the true value. In Figure 8 it can be seen that the convergence time would decrease significantly when the depth measurement is used. For the square type trajectory, there are two possible solutions for each beacon, as long as the AUV is moving on a straight line. As soon as the AUV turns, the observability condition (17) holds and the set of possible solutions for the initial condition shrinks to the true value.

4.3 Experimental Results

In this section we present the experimental results that were recently done with the three autonomous surface vehicles named Medusa vehicles (see Figure 9) which were developed at the Laboratory of Robotics and Systems in Engineering and Science (LARSyS) of the Instituto Superior Técnico, Lisbon. Each vehicle has two side thrusters that can be independently controlled. Based on the commands sent to the thrusters and the thruster model, the forward velocity $\nu(t)$ of the vehicle is calculated and used as input in the model of the AUV. Each vehicle is also equipped with an IMU and a compass which provide body orientation $\boldsymbol{\eta}(t)$ and angular velocity $\boldsymbol{\omega}(t)$ used for system model inputs. In the experiments, a pre-evaluated constant current was considered to be summed with forward velocity of the vehicle. The availability of GPS module allows us to use it for ground truth comparison purposes. The Communications from the remote console to the vehicles are done via WiFi. Moreover, each vehicle

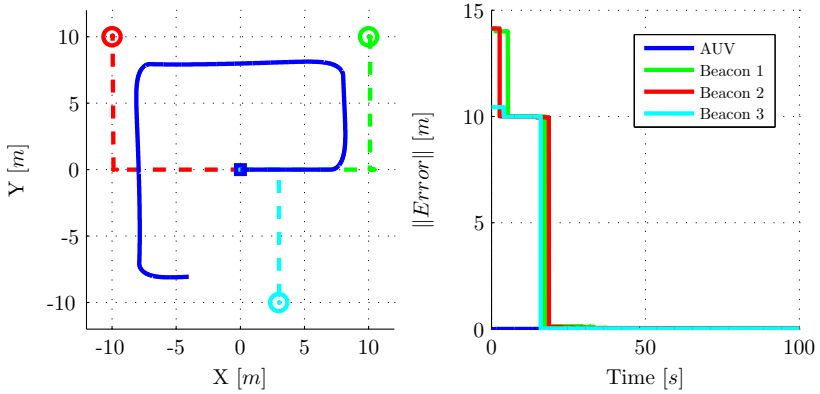

Figure 6: Evolution of the estimated position of the AUV and the beacons (left), and the norm of state estimation error (right) for the square type motion.

is equipped with an acoustic modem. Acoustic modems are used for communication between the vehicles and also ranging by acoustic signals propagation times.

To estimate the states of the model introduced in (23) we use the proposed hybrid CME combined with MMAE approach. The models in the estimator are initialized with the same initial condition but different up to a sign in initial condition ${}^{\mathcal{B}}q_{i,y}(0)$, which means that one initial condition of beacon is on the left hand side of the AUV and one at the right (see Figure 13 for an example with weighted sum of initial condition shown by (□,□)). The reason for this kind of initialization is based on the set of indistinguishable points introduced in (21), (22).

During the mission, two of the Medusa vehicles are in hold position mode to act only as stationary beacons. The moving Medusa has an average forward velocity of $0.5[m/s]$ at the surface, which starts from the initial position at (□) and interrogates with each beacon in cycles of 4 seconds. The range measurements acquired by the modems is corrupted with an additive measurement noise where after extensive trials have shown to have an standard deviation of $0.3[m]$. The moving AUV follows a lawn-mowing trajectory where observability conditions are not satisfied initially. However, as soon as the AUV turns, the observability condition (17) holds.

Figure 10 shows the Linear and angular velocities related to the mission. The internal controller of the AUV, which is doing a path-following, tries to maintain a constant speed on the track. The changes in the angular velocities of the AUV is visible when the AUV is turning.

Figure 11 depicts the trajectory of the lawn-mowing mission together with the locations of the beacons obtained by GPS (◯,◯). The estimation error converges to a bound around zero, as soon as the vehicle turns and the system becomes observable. Arbitrary chosen initial conditions do not have an effect on the convergence, since the system becomes observable and the proposed observer is globally convergent. This can also be verified from states propagation of each model depicted in Figure 13. Notice that Model 1 converges to the true locations of the beacons, while the other Models have converged to some or all

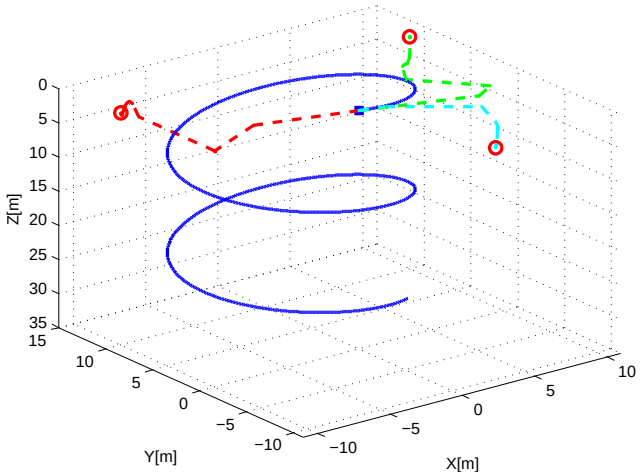

Figure 7: Evolution of the estimated position of the AUV and the beacons for the helix type motion.

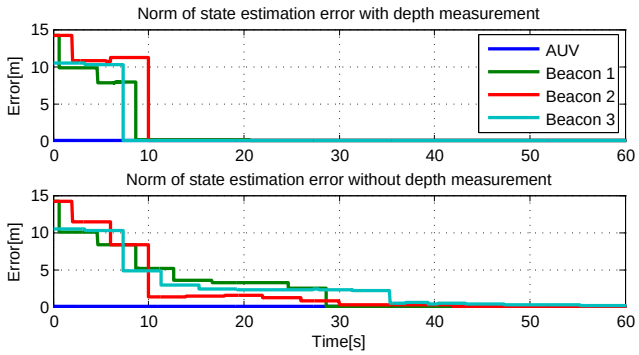

Figure 8: Evolution of the position estimation error for helix type motion with (top) and without (bottom) depth measurements.

of the mirror points for each beacon. Moreover, we could also notice that the models' weights depicted in Figure 12, converge to the model with least error function value after the observability condition is met.

In Figure 14 we compare the affect of disabling one or some of the designed blocks for all three presented missions. We consider 5 observers: i) Full designed observer consisting of the ME, PF, IOP, and MMAE; ii) Observer without the IOP module; iii) Observer without using the PF module, which solves the unconstrained problem. iv) Observer with only the ME and the MMAE module; v) Plain ME observer. As expected, the fact of taking into account the algebraic constraint together with the IOP and the MMAE along with the ME observer improves significantly the convergence and behavior of the estimation error during the transient time when compared with the unconstrained ME observer. Also notice that after convergence of the ME observer, there is not much difference between these observers. This shows that the output of the PF $\hat{\boldsymbol{x}}$ converges to the output of ME $\bar{\boldsymbol{x}}$ meaning that $\bar{\boldsymbol{x}}$ satisfies constraint (9).

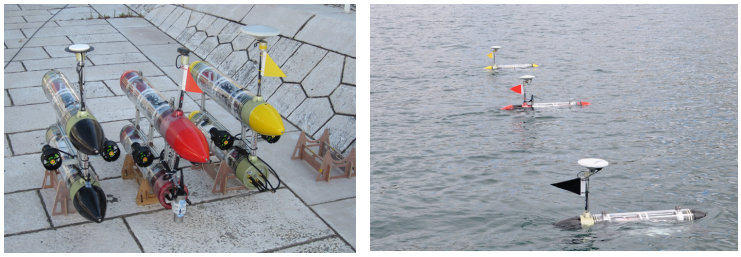

Figure 9: The three Medusa marine robotic vehicles.

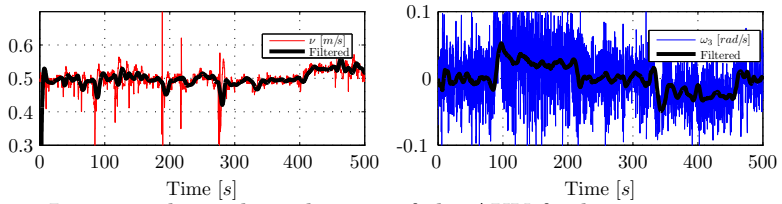

Figure 10: Linear and angular velocities of the AUV for lawn-mowing mission. Filtered data is presented with black solid line.

5 Conclusions

We addressed the observability problem of the process of simultaneously mapping the beacons locations and localizing an AUV equipped with inertial sensors, a depth sensor, and an acoustic ranging device to obtain relative range measurements to stationary beacons. We presented a convergent observer to estimate/reconstruct the states of the corresponding system (in particular initial location of the AUV). Several simulation and experimental scenarios were conducted to illustrate the observability results presented in section 3. From the derived results and experiments, it can be concluded that the observability and more precisely the set of indistinguishable points $\mathcal{I}(\boldsymbol{x}_0)$ is independent of the location of the beacons and it only depends on the motion of the AUV. Furthermore, the type of the manoeuvres performed by AUV has a direct impact on the quality of the state estimation of the system.

References

Aguiar, A. P. & Hespanha, J. a. P. (2003), Minimum-energy state estimation for systems with perspective outputs and state constraints, *in* 'Proc. 42nd IEEE Conference on Decision and Control', Maui, Hawaii.

Aguiar, A. P. & Hespanha, J. a. P. (2006), 'Minimum-energy state estimation for systems with perspective outputs', *IEEE Transactions on Automatic Control* **51**(2), 226–241.

Arrichiello, F., Antonelli, G., Aguiar, A. P. & Pascoal, A. (2011), Observability metric for the relative localization of AUVs based on range and depth measurements: Theory and experiments, *in* 'IEEE/RSJ International Conference on Intelligent Robots and Systems (IROS)', pp. 3166 –3171.

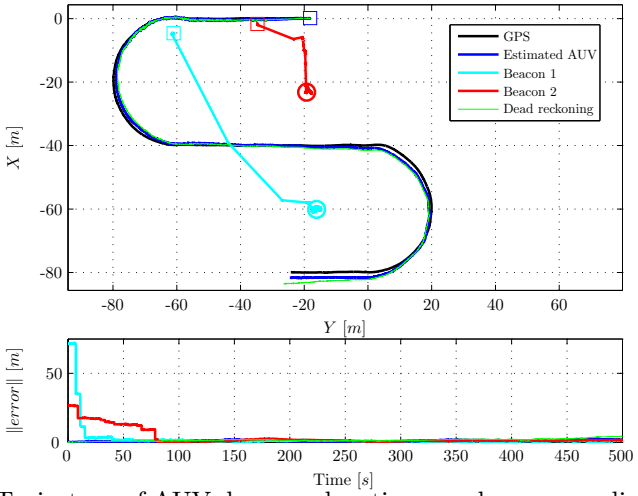

Figure 11: Trajectory of AUV, beacons locations, and corresponding estimation errors in lawn-mowing mission.

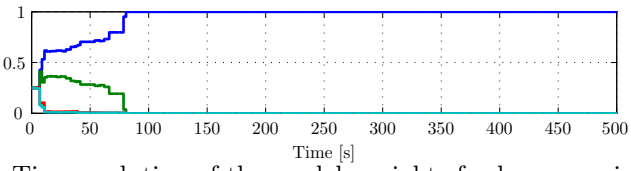

Figure 12: Time evolution of the models weights for lawn-mowing mission.

Batista, P., Silvestre, C. & Oliveira, P. (2010), Single beacon navigation: Observability analysis and filter design, *in* 'American Control Conference, Marriott Waterfront, Baltimore, MD, USA', pp. 6191–6196.

Batista, P., Silvestre, C. & Oliveira, P. (2011), 'Single range aided navigation and source localization: Observability and filter design', *Systems & Control Letters* **60**(8), 665–673.

Bayat, M. & Aguiar, A. P. (2013), Auv range-only localization and mapping: Observer design and experimental results, *in* 'European Control Conference (ECC)', Zurich, Switzerland.

Casey, T. & Hu, J. (2007), Underwater vehicle positioning based on time of arrival measurements from a single beacon, *in* 'MTS/IEEE Oceans 2007, Vancouver, BC, Canada', pp. 1–8.

Fallon, M. F., Papadopoulos, G. & Leonard, J. J. (2009), Cooperative AUV Navigation using a Single Surface Craft, *in* 'Field and Service Robots', Cambridge MA, pp. 1–10.

Gadre, A. S. (2007), Observability analysis in navigation systems with an underwater vehicle application, PhD thesis, Virginia Polytechnic Institute and State University.

Gadre, A. S. & Stilwell, D. J. (2005), Underwater navigation in the presence of unknown currents based on range measurements from a single location,

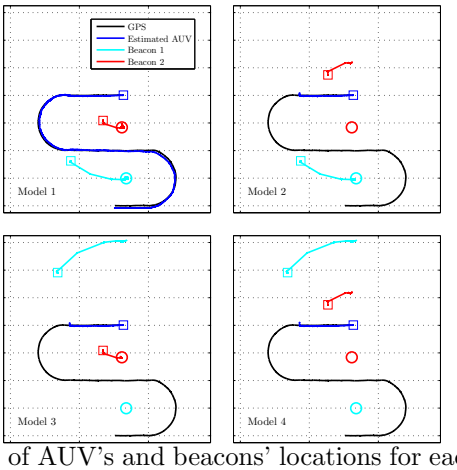

Figure 13: Evolution of AUV's and beacons' locations for each model presented in XY plane corresponding to lawn-mowing mission.

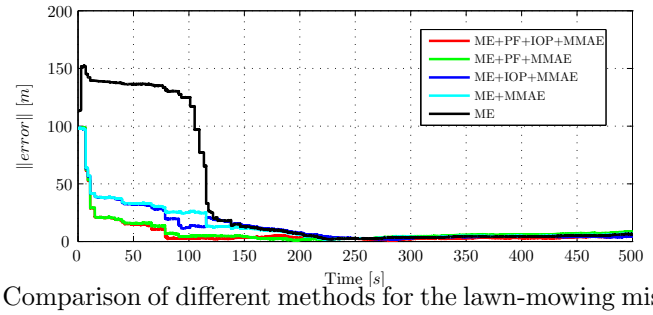

Figure 14: Comparison of different methods for the lawn-mowing mission, shown in Figure 11.

in 'Proceedings of the 2005, American Control Conference', Vol. 2, Portland, OR, USA, pp. 656–661.

Hermann, R. & Krener, A. J. (1977), 'Nonlinear controllability and observability', *IEEE Transactions on Automatic Control* **22**(5), 728–740.

Kinsey, J. C., Eustice, R. M. & Whitcomb, L. L. (2006), A survey of underwater vehicle navigation: Recent advances and new challenges, *in* 'IFAC Conference on Manoeuvring and Control of Marine Craft (MCMC)'.

Krener, A. J. & Isidori, A. (1983), 'Linearization by output injection and nonlinear observers', *Systems & Control Letters* **3**, 47–52.

Larsen, M. B. (2000), Synthetic long baseline navigation of underwater vehicles, *in* 'MTS/IEEE Conference and Exhibition OCEANS'.

McPhail, S. D. & Pebody, M. (2009), 'Range-only positioning of a deep-diving autonomous underwater vehicle from a surface ship', *IEEE Journal of Oceanic Engineering* **34**(4), 669–677.

Newman, P. & Leonard, J. (2003), Pure range-only subsea SLAM, *in* 'Robotics and Automation, 2003. Proceedings. ICRA '03. IEEE International Conference on', pp. 1921–1926.

Nijmeijer, H. & van der Schaft, A. (1990), *Nonlinear dynamical control systems*, Springer.

Olson, E., Leonard, J. J. & Teller, S. (2006), 'Robust range-only beacon localization', *IEEE Journal of Oceanic Engineering* **31**(4), 949–958.

Plestan, F. & Glumineau, A. (1997), 'Linearization by generalized input-output injection', *Systems & Control Letters* **31**, 115–128.

Saude, J. a. & Aguiar, A. P. (2009), Single beacon acoustic navigation for an AUV in the presence of unknown ocean currents, *in* 'MCMC'09 - 8th IFAC Conference on Manoeuvring and Control of Marine Craft', Guarujá (SP), Brazil.

Scherbatyuk, A. P. (1995), The AUV positioning using ranges from one transponder LBL, *in* 'MTS/IEEE. Conference on Challenges of Our Changing Global Environment OCEANS '95.', Vol. 3, pp. 1620–1623.

Song, T. L. (1999), 'Observability of target tracking with range-only measurements', *IEEE Journal of Oceanic Engineering* **24**(3), 383–387.

Webster, S. E., Eustice, R. M., Singh, H. & Whitcomb, L. L. (2009), Preliminary deep water results in single-beacon one-way-travel-time acoustic navigation for underwater vehicles, *in* 'IEEE/RSJ International Conference on Intelligent Robots and Systems (IROS)', pp. 2053–2060.

Webster, S. E., Eustice, R. M., Singh, H. & Whitcomb, L. L. (2012), 'Advances in single-beacon one-way-travel-time acoustic navigation for underwater vehicles', *The International Journal of Robotics Research* **31**(8), 935–950.